

# CHARACTERISATION OF THE SYSTEMATIC EFFECTS OF THE INSERTION DEVICES WITH PHOTON BEAM POSITION MONITORS

E. van Garderen, J. Krempaský, M. Böge, J. Chrin, V. Schlott, T. Schmidt, A. Streun  
Paul Scherrer Institut, Switzerland

## Abstract

The X-ray photo-emission monitors at the Swiss Light Source (SLS) are used for beam-position diagnostics and beam stabilization down to the sub-micron level. The main systematic change of the photon beam-position is induced by varying insertion device (ID) settings, such as photon energy, harmonic-selection or light polarization. An ID beam-position correction scheme is based on digital beam-position monitors (DBPM) located inside the storage ring, combined with analogue Bergoz BPMs, located inside the ID straight section, and analogue photon monitors (XBPMs), in beam line front-ends. The use of XBPMs in this correction scheme will be demonstrated. Moreover, in order to achieve sub-micron photon-beam stability while changing the ID parameters with XBPM-readouts requires precise XBPM alignment and characterization for each ID-setting [1-2]. We present an account of the design and performance of the XBPMs as used for characterizing systematic effects of the U19, and the more challenging elliptical undulator UE44 [3], a newly designed fixed-gap APPLE II undulator recently installed at the advanced resonant spectroscopy beam line [4].

## INTRODUCTION

The Swiss Light Source is a third-generation synchrotron radiation facility, which is in operation since mid-2001. The undulators at the SLS are working in the soft x-ray regime. By varying ID-settings such as energy and polarization of light, the angular power distribution of the synchrotron radiation changes. A blade monitor must be designed in order to provide optimal position response to different ID-settings [5]. We describe this briefly in the next section whereby the effects of light polarization of the UE44 and a gap change of U19 will be demonstrated.

The XBPM position response, given by simple signal asymmetry detection in the horizontal and vertical plane, is made by means of low-current asymmetry detectors. A graphical user interface in Fig. 1 illustrates the blade readouts  $B1$ ,  $B2$ ,  $B3$  and  $B4$  for a gap of 6 mm for U19. The horizontal and vertical positions are seen to be well aligned with the nominal beam axis. However, differences in the absolute value

of the readouts (about 12%) introduce errors in the exact determination of the beam position. These errors, determined by differences in blade resistance, impose limitations on the readout accuracy based on simple asymmetry calculation (e.g.  $(B1+B2-B3-B4)/(B1+B2+B3+B4)$  for horizontal asymmetry). For this reason the XBPM asymmetry readouts need to be calibrated. A calibration based on machine bumps is proposed below, whereby the systematic effect due to the changing in the light polarization of the UE44 will be demonstrated.

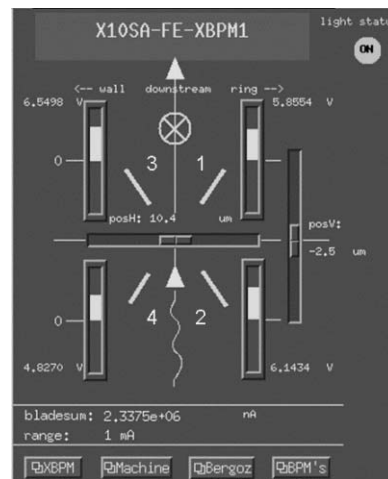


Figure 1: XBPM centered at the nominal beam axis of the U19 undulator (gap 6 mm). The horizontal ( $posH=10.4 \mu\text{m}$ ) and vertical XBPM position ( $posV=-2.5 \mu\text{m}$ ) are calculated from signal asymmetries. The signal level (V) of each blade is displayed with vertical bars.

## XBPM DESIGN FOR UE44

The total power distribution (TPD) of UE44, weighted by a detector response function of XBPM tungsten blades, is shown in Fig. 2 for linear vertical and circular polarizations [6]. A horizontal magnetic field in the electron beam induces wiggled motion in the vertical direction, which is responsible for the vertically elongated TPD. Applying the peak fields of 0.64 T in  $x$  and  $y$  direction the helical motion of the electron beam causes a “donut” shaped power

distribution, as shown in Fig. 2. The determination of the theoretical TPDs is important for the XBPM blade design.

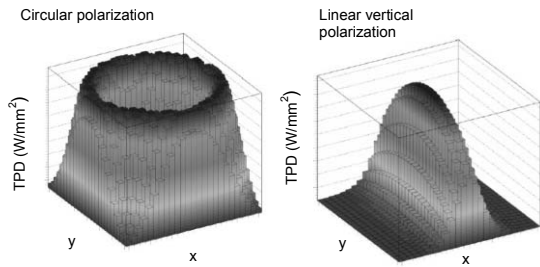


Figure 2: (color) TPD of the UE44 for circular polarizations (maximum  $1\text{E-}9\text{ W/mm}^2$ ) and linear vertical (maximum  $0.25\text{E-}8\text{ W/mm}^2$ ) [6]. The  $x$  and  $y$  scales are  $\pm 6$  mm. To reflect these TPDs, the horizontal (vertical) gap between the XBPM blades has been set to 5.2 (5.0) mm, respectively.

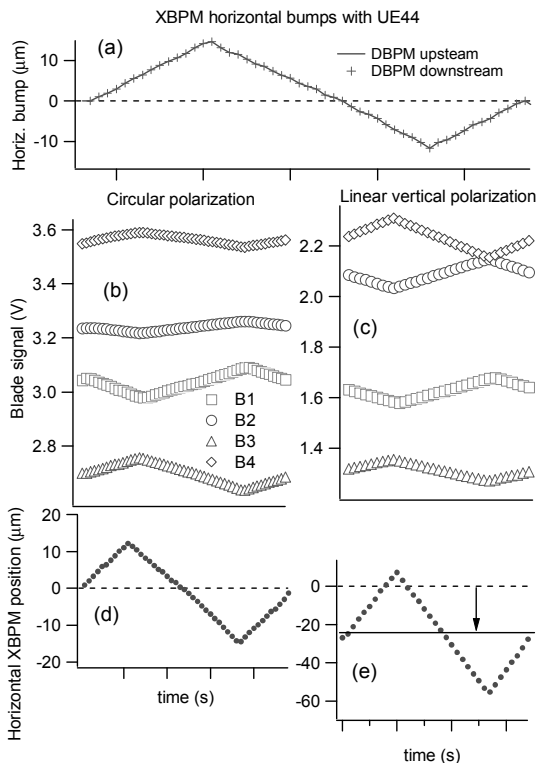


Figure 3: (color inline) XBPM response to symmetrical horizontal machine bump (a) and switching the UE44 from circular (b,d) to planar (c,e) mode. (time scale: 50 s). The shift in the horizontal photon beam excursion between the two modes is denoted by the arrow (e). The spatial assignments of XBPM blades  $B1$ ,  $B2$ ,  $B3$ ,  $B4$  is shown in Fig. 1.

## XBPM CALIBRATION WITH MACHINE BUMPS

The most direct XBPM calibration is made by means of machine bumps, which are routinely performed at SLS during fast-orbit feedback (FOFB) [7] machine operation. The XBPM response to symmetrical horizontal machine bump displacements ( $\pm 15\text{ }\mu\text{m}$ ) with FOFB is shown in Fig. 3. A time-dependency of a symmetrical horizontal bump, controlled with upstream and downstream DBPMs of the UE44 straight section, is shown in Fig. 3a. Since the XBPM has been aligned in circular mode, the beam nominal axis for this polarization is set to zero (Fig. 3d). In planar mode, the signal asymmetries change when compared to the circular mode. The response of the blade  $B2$  is an upward shift, while the other blades retain their signal level with respect to Fig. 3b. According to the blade layout in Fig. 1, this signal asymmetry change indicates a downwards-right shift in the photon beam. In the horizontal plane, this shift is well observed: the beam position is now centered  $25\text{ }\mu\text{m}$  away with respect to the circular mode. The downward photon beam shift is reflected by enhanced peak-to-peak response of the blade  $B4$ , which is also observed on vertical symmetric and/or asymmetric bumps (not shown). The factor 2 better sensitivity in vertical mode shown in Fig. 3e is given by the TPD  $2\sigma$  ratio between linear and circular mode [6].

The different signal levels relate to differences in the Ohmic resistance of the blades and could in principle be removed by introducing calibration factors (gains) for each individual blade. However, the  $\sim 25\text{ }\mu\text{m}$  shift in the horizontal photon beam centre, indicated in Fig. 3e, reflects a *systematic* shift in the horizontal beam position upon ID light polarization change. In the following, we show the influence of U19 undulator on the photon beam.

## XBPM IN INSERTION DEVICE FEED FORWARD CORRECTION SCHEME

Correction of insertion device (ID) induced orbit distortions at the SLS are performed by means of feed forward schemes (IDFF) [8] down to the micron level. The remaining orbit fluctuations are suppressed by XBPM feedbacks which are an integral part of the fast orbit feedback system (FOFB) [9]. Although the correction feedback is based on the *relative* variation of the photon-beam position, the best XBPM readout sensitivity is observed while the monitor is placed on the nominal photon-beam axis. Since all undulator XBPMs have motorized stages, it is possible to adjust their horizontal and vertical positions on-line during machine operation in order to restore the horizontal and/or vertical asymmetries for a given ID-setting. As an example, Fig. 4a shows the U19 XBPM aligned to

the nominal photon beam axis at gap 8.5 mm. Upon a gap change, and without IDFF, a horizontal beam position excursion of the order of  $\sim 150 \mu\text{m}$  is evident. An active IDFF removes this beam position excursion. It must be emphasized, that in order to obtain an IDFF performance with XBPM as shown in Fig. 4a, the XBPM must be: (i) well aligned to the undulator nominal axis; (ii) calibrated with horizontal (vertical) machine bumps for each gap. The calibration constants are derived separately for horizontal and vertical components (Fig. 4b).

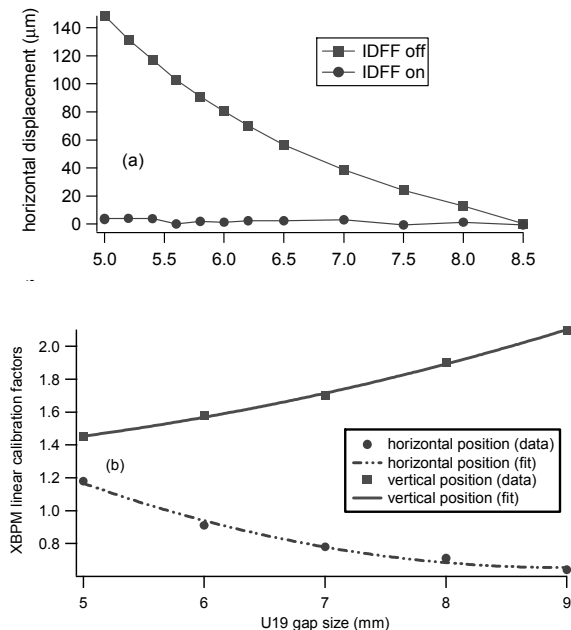


Figure 4: (color inline) (a) Systematic horizontal excursion of the U19 undulator photon beam position upon gap change. The horizontal excursion of  $\sim 150 \mu\text{m}$  (■) is suppressed owing to an active IDFF (●). (b) Horizontal (data: dots, fit: dashed line) and vertical (squares and full line, respectively) XBPM-readout calibration factors.

The significant change in the calibration factors in both horizontal and vertical directions ( $\sim 100\%$ ) during the ID-gap change shown in Fig. 4 should be noted. It has to be emphasized, that the bending magnet radiation gives a factor 100 less signal compared with the total photon flux. This can be easily checked with a *bladesum* signal  $B1+B2+B3+B4$  measured at a fully opened gap. Such undulator/bending magnet signal-to-noise ratio is achieved through optimized spatial placement of the XBPM blades [6].

## CONCLUSIONS

In summary, well designed, aligned and calibrated XBPMs are capable of accounting for the systematic photon beam position distortions induced by ID-settings variations. The orbit distortion is created by kicks at entry and exit of the ID, due to typical edge field behaviour. Two different undulator types, where light polarization and gap was changed, have been studied. In general, each ID-setting requires an XBPM calibration. XBPM calibrations based on machine bumps across the undulator straight sections are fully automatized in EPICS and are made during dedicated machine shifts at SLS. The chosen method for compensating the systematic effects of the IDs are IDFF correction tables which include the XBPM readout.

## ACKNOWLEDGMENTS

We would like to thank K. Holldack (BESSY) for useful discussions. We also acknowledge the technical support from Q. Chen and R. Wullschlaeger during the installation of the XBPMs into the front-ends.

## REFERENCES

- [1] K. Holldack et al., *Review of Emittance and Stability Monitoring Using Synchrotron Radiation Monitors*, DIPAC 2001
- [2] J. Krempasky et al., *The Use of Photon Monitors at the SLS*, EPAC 2004
- [3] <http://sls.web.psi.ch/view.php/beamlines/address>
- [4] T. Schmidt et al., *Insertion device activities*, PSI scientific report, Vol VII, 2004
- [5] J. Krempaský et al., *Insertion device photon beam studies with X-ray monitors*, proceedings EPAC 2004
- [6] K. Holldack, *SLS-UE44: On the Design of Front-End Monitors*, private communications
- [7] T. Schilcher et al., *Commissioning and Operation of the SLS Fast Orbit Feedback*, EPAC 2004
- [8] T. Schmidt, J. Chrin, A. Streun, D. Zimoch, *Feed Forward Corrections for Insertion Devices at the SLS*, PSI Scientific Report 2003, Vol. VI, 2003.
- [9] M. Böge et al., *Correction of insertion device induced orbit distortion at the SLS*, PAC 2005